



Publication Year	2022
Acceptance in OA @INAF	2024-05-07T11:34:34Z
Title	A new method for accurate calibration of solar disk emission in the radio band
Authors	MULAS, Sara; PELLIZZONI, ALBERTO PAOLO; IACOLINA, Maria Noemi; EGRON, Elise Marie Jeanne; MARONGIU, Marco; et al.
Handle	http://hdl.handle.net/20.500.12386/35089
Number	RS-UCS-2022-007



Agenzia Spaziale Italiana

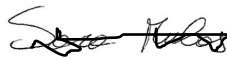
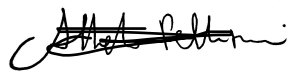
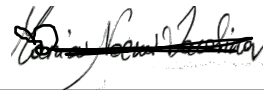
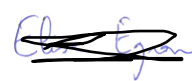

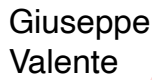


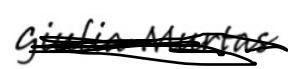
Internal Report


Document: RS-UCS-2022-007


Date: 14/09/2022

Page 1 of 35

A New Method for Accurate Calibration of Solar Disk Emission in the Radio Band

	NAME/AFFILIATION	SIGNATURE	DATE
AUTHORS	<i>Mulas S.^{1,2}</i>		14/09/2022
	<i>Pellizzoni A.³</i>		14/09/2022
	<i>Iacolina M.N.¹</i>		14/09/2022
	<i>Egron E.³</i>		14/09/2022
	<i>Marongiu M.³</i>	 MARONGIU MARCO 15.09.2022 15:14:14 GMT+01:00	14/09/2022
	<i>Valente G.¹</i>	 Giuseppe Valente Firmato digitalmente da Giuseppe Valente ND: cn=Giuseppe Valente, o=ASI, c=IT email=giuseppe.valente@asi.it, c=IT Data: 2022.09.15 08:03:36 +02'00'	
	<i>Melis A.³</i>	 MELIS ANDREA 15.09.2022 08:19:03 GMT+00:00	
	<i>Righini S.⁴</i>	 Simona Righini Firmato digitalmente da Simona Righini ND: cn=Simona Righini, o=INAF-IRA, c=IT email=simona.righini@inaf.it, c=IT Data: 2022.09.15 13:53:02 +02'00'	15/09/2022
	<i>Murtas G.⁵</i>		15/09/2022
AUTHORS AFFILIATION	¹ ASI - Cagliari Astronomical Observatory ² University of Cagliari ³ INAF - Cagliari Astronomical Observatory ⁴ INAF - Institute of Radio Astronomy, Bologna ⁵ Los Alamos National Laboratory		

 Agenzia Spaziale Italiana	Internal Report	Document: RS-UCS-2022-007 Date: 14/09/2022 Page 2 of 35
<h2 style="text-align: center;">A New Method for Accurate Calibration of Solar Disk Emission in the Radio Band</h2>		


	NAME/AFFILIATION	SIGNATURE	DATE
APPROVED	<i>Viviano S.¹</i>	 SALVATORE VIVIANO 15.09.2022 16:48:15 GMT+01:00	

Change log

Date	Document emission / revision motivation	Revision
08/09/2022	First emission / Draft	A
14/09/2022	Second emission / modification and revision by authors	B

Distribution list

- Open

 Agenzia Spaziale Italiana	Internal Report	Document: RS-UCS-2022-007 Date: 14/09/2022 Page 3 of 35
<h1>A New Method for Accurate Calibration of Solar Disk Emission in the Radio Band</h1>		

Summary

Abstract	5
1 Introduction	6
2 Solar Image Production	8
2.1 Instrumental Set-up	8
2.2 Data Processing Method	9
2.3 Observing Data	10
3 Solar Image Calibration	12
3.1 Self Calibration	12
3.2 Absolute Solar Calibration Techniques	13
4 Quiet-Sun Brightness Estimation	14
4.1 Data Analysis	14
4.2 Results	17
5 Absolute Calibration Uncertainty Study	19
5.1 Baseline Subtraction Method	19
5.2 Sky opacity contribution	20
5.3 Cas A spectral fit	21
5.4 Secular decrease formula	22
6 Calibration problems and issues	22
6.1 Early Spectro-Polarimetric Observations at Medicina	24
7 Conclusions and Future Strategies	25
Acknowledgement	27
References	30



Agenzia Spaziale Italiana

Internal Report

Document: RS-UCS-2022-007


Date: 14/09/2022

Page 4 of 35

A New Method for Accurate Calibration of Solar Disk Emission in the Radio Band

Acronym list

QS	Quiet Sun
ARs	Active Regions
LTE	Local Thermodynamic Equilibrium
SRT	Sardinia Radio Telescope
SDSA	Sardinia Deep Space Antenna
OTF	On The Fly
RA	Right Ascension
DEC	Declination
INAF	Istituto nazionale di Astrofisica (National Institute of Astrophysics)
ASI	Agenzia Spaziale Italiana (Italian Space Agency)
SNR	Supernova Remnant
Cas A	Cassiopeia A
RFI	Radio Frequency Interference
SDI	Single-Dish Imager
SDT	Single Dish Tools
FITS	Flexible Image Transport System
LNA	Low-Noise Amplifier
SUNPIT	SUNdish Pipeline Tool
SUNDARA	SUNdish Active Region Analyser


 Agenzia Spaziale Italiana	Internal Report	Document: RS-UCS-2022-007 Date: 14/09/2022 Page 5 of 35
<h2 style="text-align: center;">A New Method for Accurate Calibration of Solar Disk Emission in the Radio Band</h2>		

Abstract

The SunDish project¹ aims to map and monitor the Sun at radio frequencies with the Sardinia and Medicina Italian Radio telescopes by performing single-dish imaging observations in K-band (18-26 GHz) at present. In the future it will even be possible to exploit Ka (32.5 GHz) and X-band (8.5-9 GHz) simultaneous observations and go up to 100 GHz in order to fill the observational gap in literature and contributing to Space Weather networks.

This technical note is focusing on the original and innovative procedure for the absolute calibration of the Sun maps that we developed for the SunDish project that adopted the Supernova Remnant Cassiopeia A as a flux reference. This is a challenging procedure since this calibrator is an extended source (resolved at our frequencies) and it is currently in expansion. However, due to its strong flux, Cassiopeia A presents several advantages compared to other standard calibrators and its brightness variation is well studied in literature. We found that this Supernova Remnant is a well suited and very reliable calibrator for solar radio observations that require high signal attenuation in the instrumentation chain and consequently strong flux calibrators. Thanks to the Cassiopeia A visibility (circumpolar source) at the telescopes latitude, it is possible to obtain accurately calibrated Sun maps throughout the day with typical errors <3% in K-band.

¹<https://sites.google.com/inaf.it/sundish>

 Agenzia Spaziale Italiana	Internal Report	Document: RS-UCS-2022-007 Date: 14/09/2022 Page 6 of 35
<h1 style="text-align: center;">A New Method for Accurate Calibration of Solar Disk Emission in the Radio Band</h1>		


1 Introduction

The solar atmosphere is generally described as being composed of multiple layers, from the deepest, the photosphere, followed by the chromosphere, the transition region and the corona. The radio frequencies are a useful tool to inquire valuable information on the structure and dynamics above the temperature minimum to the low corona [38].

The solar physics science offers a rich interdisciplinary ground on astrophysics, plasma physics, nuclear physics and fundamental physics. Furthermore, the magnetic and radiative activity of our star has an enormous impact on planetary magnetospheres and ionospheres ranging from subtle climate dependencies to severe radiation phenomena affecting operations and safety of our technologies on Earth (see e.g. [15], [40]). The radio Sun can also be helpful to shed light on the problem of the heating of the chromosphere and the corona (see, e.g., [38], [1]), and study the electron plasma frequency and the electron gyrofrequency ([28]).

The solar radio emission is usually divided in the literature into three main parts depending on the time scale of the events: (1) the quiet Sun (QS) as a background stable emission, (2) a slowly varying component mostly associated with the active regions (ARs), and (3) occasional extreme and sudden energetic phenomena like coronal mass ejections and flares.

The QS brightness temperature spectrum has been modelled in several papers (e.g. [16]; [48]; [32]). Its radio emission comes from thermal bremsstrahlung in local thermodynamic equilibrium (LTE), therefore it has the advantage to be well understood and modeled compared to other frequencies. It can thus be used as a powerful diagnostic of the physical conditions and parameters in a wide range of atmospheric layers ([38]). In K-band (18-26 GHz) however, there is a lack of accurate and calibrated measurements of the brightness temperature of the QS component since it is difficult to separate it from the contribution of the ARs. The local emission in the chromospheric layers slightly deviates from simple thermal bremsstrahlung in the optically thick regime. In fact, instead of having a flux density spectral index (α) of 2, typical of a Rayleigh-Jeans emission, it assumes a value around 1.9 ([32]) due to the logarithmic dependence of the Gaunt factor on frequency. The QS emission resulting from the combination of the chromospheric layers suggests a possible spectral change from lower to higher frequencies ([16]), such as flattening. From the work of [16] the QS is predicted to have a value between 10227-9377 K in the 18-26 GHz interval, with an $\alpha = 1.76$, which is slightly lower than the value obtained by our SunDish observations ($\alpha = 1.89$, [32]), although they are compatible within errors. [16] used the data from [6] to fit the QS spectrum (see sec 3.1) at high frequencies. While [6] selected the data with the highest possible accuracy, it is known that the millimeter observations are more uncertain than the centimeter ones. In fact, it can be seen from [16] that the data from 35 GHz

 Agenzia Spaziale Italiana	Internal Report	Document: RS-UCS-2022-007 Date: 14/09/2022 Page 7 of 35
<h2 style="text-align: center;">A New Method for Accurate Calibration of Solar Disk Emission in the Radio Band</h2>		


show a large scatter, which could explain the discrepancy in the α with the [32] works which uses QS values with high accuracy.

The ARs radio emission mechanism is more difficult to understand than the QS since there is an entanglement of thermal (free-free and gyroresonance) and non-thermal emission depending on the observing frequency. In the radio domain the gyroresonance has been detected till 17 GHz (see [28] and references therein), and has its emission peak in the 2-5 GHz range ([12]; [27]). At higher frequencies (from 34 GHz) the ARs emission has been modeled as purely free-free ([37]), and in the range between 212-405 GHz, [39] as thermal bremsstrahlung. Taking into consideration the ARs flux density spectra from [39], the K-band seems to be a transition region between different emission mechanism. In the [32] work both positive and negative α values are associated to the ARs in the 18-26 GHz interval. This complexity confirms that it is a not trivial task to understand the emission mechanism in the K-band. Regarding the peak of the excess brightness temperature above the QS, [32] found that in the K-band varies between $\sim 10^2$ and $\sim 10^3$ K.

The ARs can sometimes host a flare, a powerful event consisting in a large eruptions of electromagnetic radiation. The apparent characteristics of a solar flare can change depending on the observing frequency, the spatial and time resolution of the instrument used. However, there are some general characteristics that can still be deduced from the observed time variation of the electromagnetic radiation. A flare can, in general, be roughly divided into three phases: Precursor, Impulsive Phase and Gradual Phase [14]. These three phases do not necessarily occur in all flares and some of them could be not detectable at certain radiation frequencies. [4] reports the brightness temperature expected from a flare and the main emission mechanism involved, depending on the wavelength range: in the mm-m range from 10^6 to 10^{10} K mainly from gyrosynchrotron radiation; in the cm-dm range up to 10^{15} K from cyclotron maser; in the dm-km range up to 10^{17} K from plasma radiation. However, this very strong and point-like emission is diluted in the radio beam of relatively low-spatial resolution instruments (see [32]).

Aside from the previous emission components, [13] studied the semi-active feature, an activity present in the radio domain even when the Sun appears ostensibly quiet at 37 GHz. In the study, they observed during the solar minimum, when the ARs were not present in the disk. The semi-active feature were found to have, at maximum, an excess above the QS level of 250 K, and for almost every sources, they found a counterpart in the EUV data. In [32] similar rich network structures were detected at 18-26 GHz on much larger scales of a typical AR, which were considered compatible with the semi-active feature described by [13].

In order to obtain valuable information on the structure of the solar atmosphere above the temperature minimum with the radio data, there is the need of reliable absolute measurements of the brightness

 Agenzia Spaziale Italiana	Internal Report	Document: RS-UCS-2022-007 Date: 14/09/2022 Page 8 of 35
<h2 style="text-align: center;">A New Method for Accurate Calibration of Solar Disk Emission in the Radio Band</h2>		

temperature. Single-dish radio imaging ([38], [32]) represents the most suitable technique to perform accurately calibrated observations, due to inherent difficulties to calibrate solar interferometric images. We provided a catalog of radio continuum solar imaging observations with Medicina 32-m and SRT 64-m single-dish radio telescopes, including the multi-wavelength identification of active regions, their brightness and spectral characterization in [32]. This internal report describes in detail the solar absolute calibration procedure used in the article.

In sec 2 we illustrate the instrumental set-up needed to perform solar observations with the radiotelescopes, the software implemented for the analysis and the data acquired. In sec 3 we describe the different methods used to calibrate our maps, in particular the absolute calibration technique. This method exploits the Supernova Remnant Cassiopeia A as an external calibration source as explained in more details in sec 4. In the same section we report the Quiet Sun calibrated measurements obtained after the implementation of the procedure. The sec 5 is focused on the analysis of the most important error sources we encountered in the absolute calibration procedure. In sec 6 we give a description of the unusual and unexpected changes in the Quiet Sun absolute calibration calculations obtained from the beginning of 2021 and investigate their possible origins. Finally, in sec 7 we presents our conclusions and plans for future observations.

2 Solar Image Production


2.1 Instrumental Set-up

In order to perform the solar radio observations, we used two single-dish antennas from the INAF radio telescopes network²: the 64-m Sardinia Radio Telescope (SRT) [36] and the 32-m antenna at Medicina. The SRT is also operated by the ASI for spacecraft tracking and space science (Sardinia Deep Space Antenna, SDSA [7]). The solar maps were acquired through On-the-Fly (OTF) scans. This observing mode differs from Raster scans since the data acquisition is continuously ongoing while the antenna performs constant-speed scans across the sky, instead of tracking individual points. Usually, it produces alternatively maps along the Right Ascension (RA) and Declination (Dec) directions ([36]).

Both the SRT and the Medicina Radio Telescope were not initially designed to perform solar image observations, therefore, from 2018 the team has started developing an imaging configurations for solar observations with both instruments in the 18–26 GHz frequency range (SunDish project³, in collaboration with INAF and ASI; [33]; [9]; [35], [32]). For our data we used the cryogenic dual-

²<https://www.radiotelesopes.inaf.it>

³<https://sites.google.com/inaf.it/sundish>.

 Agenzia Spaziale Italiana	Internal Report	Document: RS-UCS-2022-007 Date: 14/09/2022 Page 9 of 35
<h2 style="text-align: center;">A New Method for Accurate Calibration of Solar Disk Emission in the Radio Band</h2>		

polarisation 7-beam K-band receiver (18–26.5 GHz, Gregorian focus; [43], [29], [42], [41], [26], [19], [25]). The radio signal is processed through the SARDARA system, a full-stokes spectral-polarimetric ROACH2-based back-end with 1.5 GHz bandwidth ([23]).

In K-band, the solar brightness is over three orders of magnitude higher than typical radio-astronomical calibration sources ($\sim 5000 \text{ Jy/arcmin}^2$). The implementation of variable attenuators for additional signal attenuation, included in the receivers' amplification chain, was crucial to avoid electronic saturation in signal response and possible instrumental damage.

The experimental solar observations, taken on about weekly basis in the last years, have helped to establish the Italian radio telescope network as a non-dedicated solar imaging facility. In the beginning of 2022 the first article from the SunDish team was published in Solar Physics ([32]), in which the implementation of the instrumental configurations for radio-continuum solar imaging and the observing techniques adopted for the solar observations is described in detail.

2.2 Data Processing Method

In order to produce our images we used the SRT Single-Dish Imager (SDI), an IDL (Interactive Data Language⁴) tool designed to perform continuum and spectro-polarimetric imaging for most receivers back-ends available for INAF radio telescopes (see details and applications in [5], [19], [33], [21], [18], [20] and [32]). The output files are generated as FITS images, which are suited to be further analyzed with standard astronomy tools.


SDI performs an automated baseline subtraction of radio background scan by scan, using different methods adapted to each specific imaging target (see [5, 19, 18]). For the solar maps we adopted a simple yet robust method: a linear approximation of the baseline taken by connecting the minimum values at the beginning and at the end of the scan. For Cas A instead we used a more sophisticated baseline subtraction method due to the lower source signal (see e.g. [5], [19]).

The K-band is influenced by a few RFI, however the sky opacity takes an important role in the final quality of the maps. The opacity can come from different sources: the Ionosphere, the Troposphere, transient events such as clouds and fog [24]. Even without clouds and rain, the absorption and re-emission of microwave radiation is significant above 20 GHz, with a peak at 22.235 GHz in correspondence to the water vapor absorption line [46].

SRT is equipped with an atmospheric monitoring and forecasting system [2] mainly composed of a local area model based on the Weather Research and Forecasting Model⁵ and a microwave radiometer.

⁴<https://www.l3harrisgeospatial.com/Software-Technology/IDL>

⁵<https://www.mmm.ucar.edu/weather-research-and-forecasting-model>

 Agenzia Spaziale Italiana	Internal Report	Document: RS-UCS-2022-007 Date: 14/09/2022 Page 10 of 35
<h2 style="text-align: center;">A New Method for Accurate Calibration of Solar Disk Emission in the Radio Band</h2>		

The first one gives the atmosphere and weather forecast every 3 hours starting from 00:00 UT up to 48 hours in advance. The latter, provides real-time radiometer data at different time intervals from 1 to 100 GHz. For our calculations we decided to use the values from the radiometer, because even if the theoretical model gives values at a more precise frequency, the data are characterized by a large bandwidth, therefore we gave priority to a value with a more precise time interval. The only exception was the 29/10/2020 data since the radiometer was malfunctioning. We used a normalized gain curve with a τ factor to correct the raw counts before the calibration procedure and take into account not only the gain loss due to target elevation, but also the weather conditions.

To cross check the data and the results, we used a new Python package version designed for the quicklook, imaging and analysis of single-dish radio data with SRT, called SRT Single Dish Tools (SDT, also publicly available for data processing⁶) and SUNDARA (SUNDish Active Region Analyser), a Python Package aimed at the automatic data analysis of solar images processed by SDI and/or SDT [22], [20]

2.3 Observing Data

We performed several observing session tests and obtained the maps of the Sun and Cas A with SRT (see Fig 1) listed in Tab. 1 and Tab. 2 at three different central frequencies: 18.8, 24.7 and 25.5 GHz.

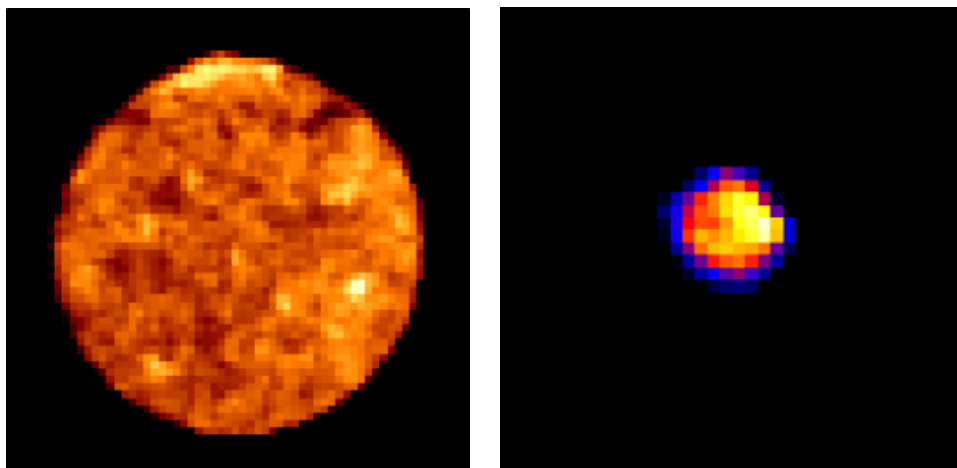


Figure 1: Example of a Sun and a Cas A images acquired with SRT at 18.8 GHz on 09/10/2019.

⁶<https://srt-single-dish-tools.readthedocs.io/en/latest/>

Table 1: List of the solar maps acquired with SRT analysed in this work

Epoch (DD/MM/YYYY)	Time (UT)	Freq (GHz)
29/10/2020	10:17-12:01	18.8
09/10/2019	11:46-13:30	18.8
09/10/2019	09:14-10:58	24.7
17/05/2019	08:40-10:24	25.5
17/05/2019	10:25-12:10	25.5

Table 2: List of the Cas A maps acquired with SRT analysed in this work

Epoch (DD/MM/YYYY)	Time (UT)	Freq (GHz)
29/10/2020	12:07-12:56	18.8
29/10/2019	13:21-13:59	18.8
09/10/2019	13:40-14:37	18.8
09/10/2019	14:41-15:40	24.7
17/05/2019	13:03-14:08	25.5

We performed another session on 28/01/2020, but the maps showed some kind of unexpected error in the synchronization of the celestial coordinates for some pixels (Fig 2)

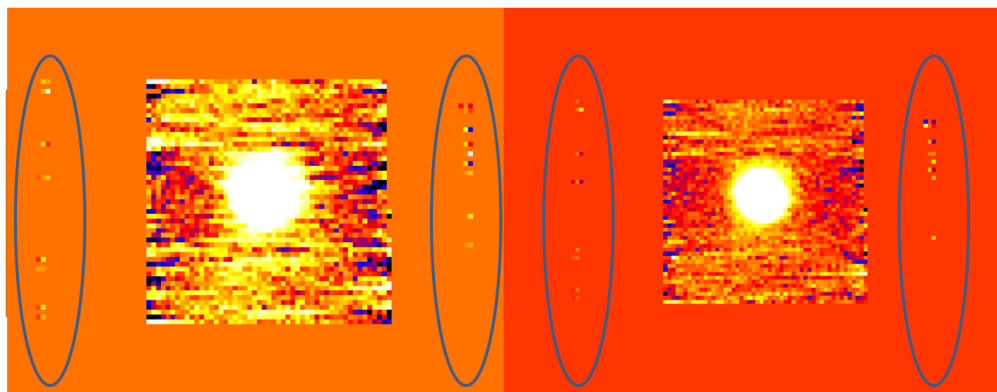



Figure 2: Synchronization problems of the celestial coordinate for some pixels outside the map boundaries in a Cas A image acquired on the 28/01/2020 at 18.8 Ghz.

 <p>Agenzia Spaziale Italiana</p>	<p>Internal Report</p>	<p>Document: RS-UCS-2022-007 Date: 14/09/2022 Page 12 of 35</p>
<p>A New Method for Accurate Calibration of Solar Disk Emission in the Radio Band</p>		

3 Solar Image Calibration

The raw images acquired with the INAF radio telescope are obtained in counts, an electronic measurements given by the back-end in use proportional to the flux density. In order to obtain a map expressed in a physical quantity (flux density or brightness temperature), there is the need to observe a calibration source – a celestial object with a flux density, or brightness temperature, well known and studied in the literature – to calculate the conversion factor from counts to a physical unit of measurements. This factor is obtained by comparing the raw counts of the calibration sources with the theoretical flux, and it is calculated for each observing session since the counts value depends on various factors (e.g. the attenuation set up, the sky opacity, or the meteorological conditions).

Among different techniques and sources used to perform the calibration procedure, we used two different approaches: the so-called self and the absolute calibration. The first method compares the average raw counts in the image from the QS with literature data and published brightness information. The latter, exploits an external source for the comparison. The instrumental setup for solar observations requires several additional signal attenuation compared to non-solar radio telescope operations (see sec 2.1). For this reason the standard calibrators ([34]) are not the ideal source, since their flux is typically low. Therefore, in order to obtain accurate measurements with the absolute calibration, we implemented a new procedure using the young and strong supernova remnant (SNR) Cassiopeia A (Cas A). Compared to the standard calibrators, which are stable point like sources, Cas A is extended at our frequencies of interests and it is still expanding and changing. However its evolution is well studied in literature (see e.g. [44]), therefore easily to predict.

3.1 Self Calibration

As said in the previous paragraph, a possible way to calculate the count-to-Kelvin conversion factor is the self-calibration method. In order to accurately estimate the average counts from the QS we used a Gaussian fit of the image histogram (counts distribution among pixels) extrapolated from the solar maps as the example reported in Fig. 3. In some cases a Johnson’s S_U -distribution [11, 10] would provide a better fit of the QS brightness distribution with respect to the Gaussian shape, however this latter approximation does not significantly affect the calibration process [32]. We calculated a negligible error of 0.02% in the estimation of the average QS counts. Therefore, we adopted the Gaussian fit in our data processing pipeline for the entire data set for simplicity.

For this calibration method our brightness reference from the literature comes from [16]. This work observed a break in the spectrum at about 10 GHz, which corresponds to a brightness temperature of about 12,000 K referred to the center of the solar disk. They obtained a spectral fit ($\chi^2 = 0.032$) for

A New Method for Accurate Calibration of Solar Disk Emission in the Radio Band

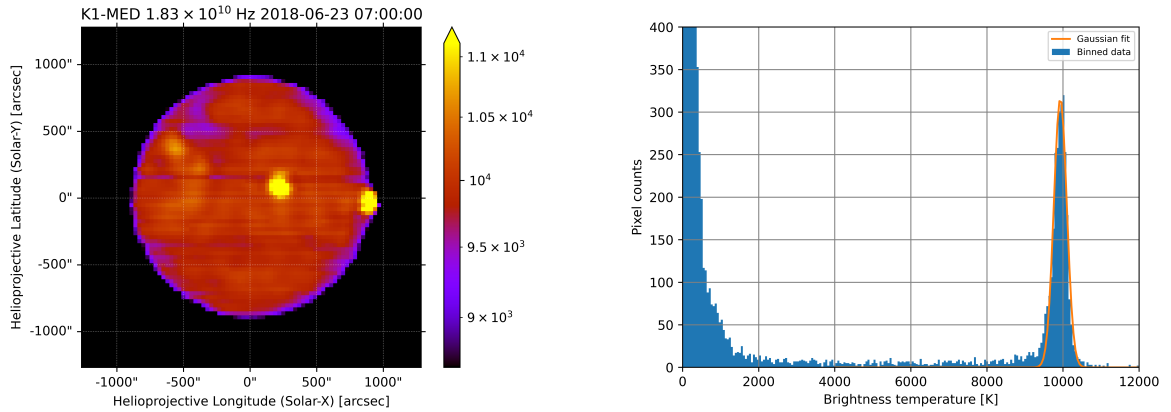


Figure 3: Left panel: Total intensity map of the solar disk at 18.3 GHz acquired with the Medicina Radio Telescope on 23-Jun-2018. Right panel: histogram of brightness distribution among pixels of the solar map and estimation of the average counts from the QS using a Gaussian fit (orange line) (credits [32]).

frequencies above 10 GHz characterized by a logarithmic linear relation between the brightness (T_b , in units of Kelvin) and the frequency (ν , in units of Hz):

$$\log_{10}(T_b) = a + b \times \log_{10}(\nu) \quad (1)$$


where $a = 6.43$ and $b = -0.236$. [16] do not provide a fit error estimate, but the measurements used in their model are typically affected by $\sim 5\%$ errors in the 10-20 GHz range and a much larger measurements spread is present above 30 GHz.

Although the self calibration is a reliable method to obtain the QS value, it is worth noting that there is a lack of calibrated measurements in literature in the 18-30 GHz range in [16].

3.2 Absolute Solar Calibration Techniques

As mentioned previously, the absolute calibration procedure exploits an external source in order to find the conversion factor from counts to Jy (or K). In some cases, the Moon has been chosen as the calibration source: in the work of [39] the brightness temperature of the QS and ARs were calibrated against observations of the new Moon by using the values from [17]. Also in the work of [6] the new Moon brightness spectrum was used to calibrate the observations.

The 18-26 GHz range has few external inferences while the sky opacity plays a fundamental part

 Agenzia Spaziale Italiana	Internal Report	Document: RS-UCS-2022-007 Date: 14/09/2022 Page 14 of 35
<h2 style="text-align: center;">A New Method for Accurate Calibration of Solar Disk Emission in the Radio Band</h2>		

in the image final quality [2]. An ideal calibration source should be subjected to similar sky opacity condition as the main source, in order to minimize the error due to the opacity τ . The New Moon could have been a possible calibration source, however it was not easy to meet suitable visibility conditions of the Sun and the Moon for our observing sessions. Accordingly, we searched for a bright celestial object visible during the solar sessions which could be observed with the same solar attenuation configuration while preserving a linear dynamic range. As we excluded that the standard point-like sources can fulfill this requirement, we adopted the SNR Cas A (Fig 1 right panel) for our solar observations.

This source is a young SNR, first discovered by the British astronomers Sir Martin Ryle and Graham Smith in 1948 ([3]), probably coming from a Supernova seen in 1670 ([47]). It is one of the best studied remnant, which represents a reach laboratory for investigating the early evolutionary phase of SNRs. Several papers have been made in order to study, for example, its morphology, expansion rate, SNe–SNRs connection, and 3D structure characterization (see [30] and correlated papers).


This SNR presents several advantages as a radio calibrator. First of all, it is a strong radio source with a flux up to 10^3 Jy in the microwave domain and comparable to the radio flux of the QS at meter wavelengths ([3]). In K-band the extrapolated flux from the [44] fit indicates a flux range from 249 to 198 Jy at the beginning of 2020 epoch with a spectral index of $\alpha = -0.71$. Moreover, it is circumpolar at the SRT and Medicina radio telescopes latitudes, therefore we can acquire the data from both the Sun and the calibrator during the same observing session. In K-band, Cas A has a almost circular shape with a radius of about 5 arcmin.

4 Quiet-Sun Brightness Estimation

The use of the extended SNR Cas A as a solar calibrator is a new method introduced for the first by our group [32]. We first calibrated the QS of each maps at the different frequencies and compare our results with the value from [16] in order to verify its trustworthiness.

4.1 Data Analysis

We used the imaging tool SDI and paired the calibrators and Sun maps at the same frequencies and epoch. For example, on the 29/10/2020 we have two Cas A maps at 18.8 GHz and one solar map at the same frequency. We obtained two different values of QS using the two calibrator maps on the same solar image. In the opposite case, e.g. on the 17/05/2019, we have two solar maps and only one Cas A image. We again, obtained two different values for the QS by pairing the calibrator map with the two different target images. The steps needed to obtained the value of the calibrated QS with the SDI

 Agenzia Spaziale Italiana	Internal Report	Document: RS-UCS-2022-007 Date: 14/09/2022 Page 15 of 35
<h2 style="text-align: center;">A New Method for Accurate Calibration of Solar Disk Emission in the Radio Band</h2>		


pipeline are the following:

- generate a Cas A quicklook map by executing the command `sd_ql`;
- extrapolate the total counts from the left and right circular polarized images of Cas A with the program SAOImageDS9. One must use the same extracting region for both channels in order to obtain a coherent result. In order to obtain coherent measurements on the QS values, we decided to use *standard* extracting regions depending on the frequency, which are reported in Tab. 3;
- produce a Sun quicklook map by executing the command `sd_sun_ql`;
- without moving the file from the working directory, the user should run the command `.r sd_sun_abscale_SaraM.pro`;
- once compiled, the user can launch the program `sd_sun_abscale_SaraM, c_freq, counts_0, counts_1, epoch, CasA_pixel`, where *c_freq* is the central observing frequency expressed in GHz, *counts_0* and *counts_1* are, respectively, the Cas A total counts extrapolated from the left and right circular polarization image, *epoch* refers to the exact time at which the observing session has taken place, and finally *CasA_pixel* is the dimension of the Cas A map pixel expressed in arcmin. It is important to note that the program takes into account the most recent input parameters file uploaded with the command `sd_init, 'inputpars_file'`;
- if the procedure has been executed correctly, the QS value for the left and right circular polarizations, and the total intensity will be printed in the terminal.

If the users want to upload a new `inputpars_file`, they should run again the `sd_init, 'inputpars_file'` command and compiled again the program `sd_sun_abscale_SaraM.pro`.

To obtain the calibrated map in units of brightness temperature (T_{bi}), it should be taken into account that in K-band the SNR Cas A appears as an extended source, so the absolute calibration procedure utilizes slightly different equations compared to a more traditional procedure with a point-like calibration source. The final expression written in our pipeline (Eq 9) is not an intuitive formula, therefore in the following its mathematical derivation is described. The maps are produced in counts per beam as a default value. However, from a scientific point of view we are more interested in a map expressed in counts per pixel, so to have, after the calibration, the precise flux contained in each map pixel. The passage from the two unit of measurements involves the ratio between the beam solid angle (Ω_{bm}) and the pixel solid angle of the map (Ω_{pix}):

$$C_i^{pix} = \frac{\Omega_{pix}}{\Omega_{bm}} C_i^{bm} \quad (2)$$

 Agenzia Spaziale Italiana	Internal Report	Document: RS-UCS-2022-007 Date: 14/09/2022 Page 16 of 35
<h2 style="text-align: center;">A New Method for Accurate Calibration of Solar Disk Emission in the Radio Band</h2>		

where C_i is the source counts for each pixel i in the image and pix or bm indicate if the counts are expressed over a pixel or over a beam. From Eq. 2 it can be seen that $\sum_i C_i^{bm} \neq \sum_i C_i^{pix}$. These relations are valid for both Cas A and the Sun.

$$C_i^{CApix} = \frac{\Omega_{pix}^{CA}}{\Omega_{bm}} C_i^{CAbm} \quad (3)$$

$$C_i^{SUNpix} = \frac{\Omega_{pix}^{SUN}}{\Omega_{bm}} C_i^{SUNbm} \quad (4)$$

where CA and SUN refer to the Cas A and Sun quantities.

We obtain the flux (Jy) contained in each pixel of a Sun map (S_i^{SUN}) by multiplying each pixel counts with the conversion factor (f), defined as the ratio between the total Cas A flux from the literature (S_{tot}^{CA}) and the the Cas A total counts expressed per pixel (C_{tot}^{CApix})

$$S_i^{SUN} = f C_i^{SUNpix} = \frac{S_{tot}^{CA}}{C_{tot}^{CApix}} C_i^{SUNpix} \quad (5)$$

If we express again the counts per pixel in counts per beam by using Eq 4, we obtain a formula where the beam solid angle is not needed anymore:

$$S_i^{SUN} = \frac{S_{tot}^{CA}}{C_{tot}^{CAbm}} \frac{\Omega_{bm}^{CA}}{\Omega_{pix}^{CA}} \frac{\Omega_{pix}^{SUN}}{\Omega_{bm}} C_i^{SUNbm} = \frac{S_{tot}^{CA}}{C_{tot}^{CAbm}} \frac{\Omega_{pix}^{SUN}}{\Omega_{pix}^{CA}} C_i^{SUNbm} \quad (6)$$

To obtain the brightness temperature in each pixel (T_{bi}) we use the Rayleigh-Jeans approximation:

$$T_{bi} = \frac{c^2}{2 \nu^2 k_B \Omega_{pix}^{SUN}} S_i^{SUN} \quad (7)$$

where c the light speed, ν is the observing frequency and k_B the Boltzmann's constant. By combining Eq 6 with Eq 7:

$$T_{bi} = \frac{c^2}{2 \nu^2 k_B \Omega_{pix}^{SUN}} \frac{S_{tot}^{CA}}{C_{tot}^{CAbm}} \frac{\Omega_{pix}^{SUN}}{\Omega_{pix}^{CA}} C_i^{SUNbm} \quad (8)$$

we can see that the information on the Sun pixel solid angle of the map is no longer necessary. Finally, we obtain the final formula we use in our solar pipeline

$$T_{bi} = \frac{c^2}{2 \nu^2 k_B} \frac{S_{tot}^{CA}}{C_{tot}^{CAbm}} \frac{C_i^{SUNbm}}{\Omega_{pix}^{CA}} \quad (9)$$

All the values expressed in Eq 9 can be found directly from the literature or through our data, except from S_{tot}^{CA} . There are no calibrated empirical measurement at our frequency. In addition, the source is in continuous expansion. As the SNR evolves, its flux decrease appreciably over a short period of time, only a few years.

In order to obtain the theoretical flux to compare with the counts from the maps, we took two steps: we extrapolate the flux at our frequencies from a model [44] and then we recalculate the value at our epoch of interest. The Cas A fit was obtained by gathering empirical value of the SNR flux from different works that cover several decades and frequencies from MHz to GHz (for further information, see [44]). All the values were brought to a standard epoch (2015.5) by using a formula which expresses the secular variation of the radio flux of Cas A in function of the frequency:

$$d_\nu [\%year^{-1}] = -(0.63 \pm 0.02) + (0.04 \pm 0.01) \ln(\nu) + (1.51 \pm 0.16) \cdot 10^{-5} (\nu)^{-2.1} \quad (10)$$

where the frequency ν is expressed in GHz and \ln indicates the natural logarithm. The final expression they obtained for the fitted curve of the Cas A spectrum at the 2015.5 epoch is:

$$S_\nu^{CasA}(2015.5) = S_0 \nu^{-\alpha + \beta \log_{10} \nu} e^{-\tau_0 \nu^{-2.1}} \quad (11)$$

where $S_0 = 2190.294 \text{ Jy} = S_{\nu=1 \text{ GHz}}^{CasA}(2015.5)$, $\alpha = 0.752$, $\beta = 0.0148$ and $\tau = 6.162 \cdot 10^{-5}$.

Table 3: Standard selection region for each central frequency (ν_{obs}). The *center* is indicated in Right Ascension and Declination coordinates while the *radius* of the circular region is expressed in degree

ν_{obs} [GHz]	Center [AR/Dec]	Radius [°]
18.8	23:23:27.567 +58:48:43.424	0.1234114
24.7	23:23:27.310 +58:48:49.582	0.1357700
25.5	23:23:25.094 +58:48:38.732	0.1199118

4.2 Results

In Fig 4 and Tab 4 the QS absolute calibration values obtained after the implementation of the procedure are reported. The errors were calculated taking into account different contribution sources (see sec 5) and they were propagated appropriately in order to calculate the final value for each frequency.

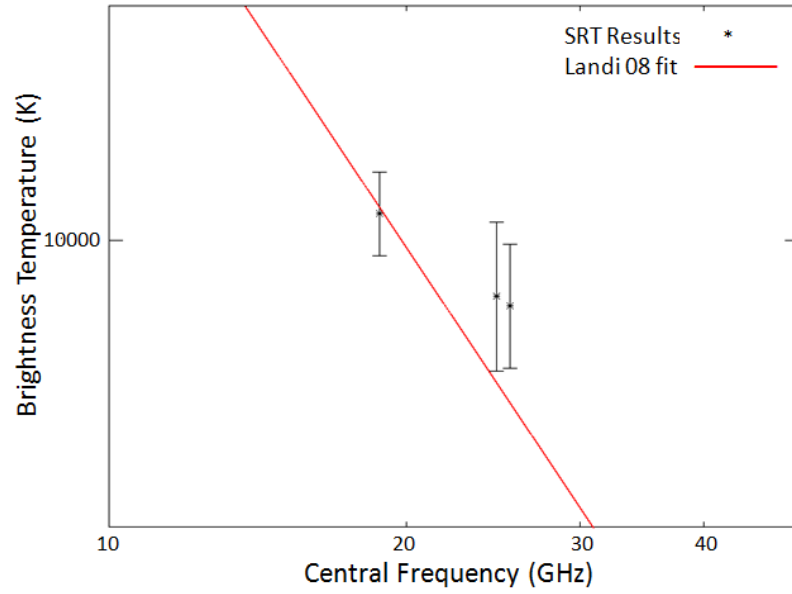



Figure 4: SRT value obtained with the absolute calibration procedure (asterisks) compared to the [16] fit (red line).

Table 4: QS brightness levels obtained from the absolute calibration procedure; ν_{obs} is the central observing frequency; $Cas A_f$ lists the SNR Cassiopeia A integrated fluxes (and related observation epochs); T_{QS} is the measured QS brightness temperature; Err lists the percentage and absolute error obtained after our calculations; Fit_{dev} expresses the deviation from the expected value extrapolated from [16] in percentage and in K.

ν_{obs} [GHz]	$Cas A_f$ [Jy]	T_{QS} [K]	Err [%]	Err [K]	Fit_{dev} [%]	Fit_{dev} [K]
18.8	247.9 ± 5.7 (Oct–2020)	10099	1.53	154	0.24	24
24.7	205.3 ± 4.8 (Oct–2019)	9799	2.74	268	3.24	308
25.5	201.1 ± 4.7 (May–2019)	9764	2.28	223	3.65	344

Our measurements are in well accordance with the fit from [16], with a maximum deviation of 3.7% and a mean relative error of 3% of our measurements for all the investigated frequencies. We are within 2σ of deviation from the theoretical values.

The deviation from the [16] work at the higher frequencies could be explained in different ways. We may need better weather condition during the observation, since the radio wave absorption is more

 Agenzia Spaziale Italiana	Internal Report	Document: RS-UCS-2022-007 Date: 14/09/2022 Page 19 of 35
<h2 style="text-align: center;">A New Method for Accurate Calibration of Solar Disk Emission in the Radio Band</h2>		

important at 25.5 and 24.7 GHz ([46]). In alternative, the deviation could be of physical origin. In the work of [16] there is a lack of empirical measurements in the K-band and the measurements at higher frequencies are more scattered than those at lower frequencies (10-20 GHz interval). As said in the Sec 1, the data from [6] (above ~ 35 GHz) were carefully selected, but they could not provide an accurate measure of the QS ([16]) resulting in the large scattering. With more precise data we managed to better constrain the QS value suggesting a flatter trend in the spectrum at high frequencies compared to the fit. However, our measurements are within 2σ from the theoretical brightness temperature. More data are needed to confirm if the deviation from the [16] fit is significant at 24.7 and 25.5 GHz.

At 18.8 GHz we have an almost perfect accordance with the theoretical value and the smaller relative error. For this frequency we had more QS calibrated values and the weather conditions had a lower impact on our final results.

In general, the deviation within 2σ of our measurements from the [16] work, is a strong indicator of the trustworthiness of our method of using Cas A as a solar calibrator source.

5 Absolute Calibration Uncertainty Study


The absolute calibration procedure is a complex method which involves several non-trivial passages. There are several kind of error sources to take into consideration, having a different impact on the final results that need an accurate assessment. In the following sections, we are going to analyse the most important error sources.

5.1 Baseline Subtraction Method

As described in section 2.2, we used an automated tool with a linear approximation in order to perform the baseline subtraction. If the background is not successfully eliminated in the Cas A map, the final QS value would be subjected to an error, since an excess amount of counts would be included in the conversion factor expressed in Eq 5, leading to an underestimation and error in the final QS evaluation.

To quantify the uncertainty induced by the procedure, we performed again the QS absolute calibration measurement adopting different baseline subtraction parameters. In this case the Cas A extracting region included as much background as possible (e.g. Fig 5 right panel) and compare the result with Tab 4. In an ideal case, the background has a zero mean, within the errors, therefore the counts from the background should not lead to a remarkable change in the QS final value.

For some maps it worked fairly well, the error on the QS measurements was less than 1%. However, for others, this value went up to 7%, which indicated that we needed a more precise algorithm. We

 Agenzia Spaziale Italiana	Internal Report	Document: RS-UCS-2022-007 Date: 14/09/2022 Page 20 of 35
<h2 style="text-align: center;">A New Method for Accurate Calibration of Solar Disk Emission in the Radio Band</h2>		

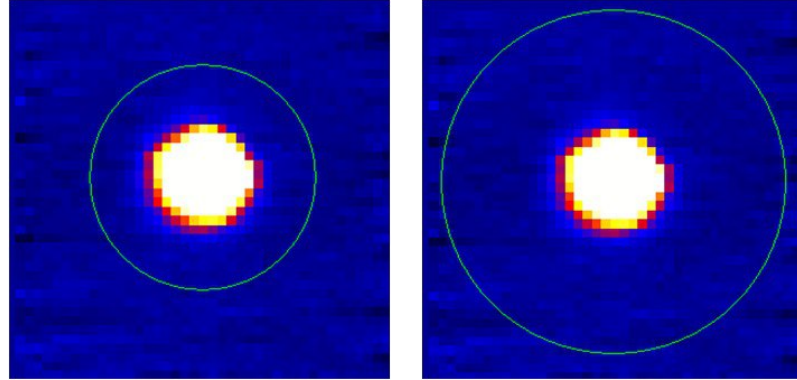


Figure 5: comparison of different extracting regions on the same Cas A map (29/10/2020 at 18.8 GHz, Feed 0 left circular polarization): left panel a standard region from 3, right panel a region with as much background as possible.

introduced a more refined baseline subtraction procedure, with a series of iteration in order to identify better the linear approximation of the baseline. This method led to a decrease in the error on the QS measure, which varies from 0.24% to a maximum of 1.56%. We tried to use further more refined iterative methods, but they did not improve significantly the final result.

The results indicated in Tab 4 were obtained with the improved baseline subtraction method.

5.2 Sky opacity contribution

As said in section 2.2, the K-band is influenced by several atmospheric and environmental factors that contribute to the signal attenuation (see [24], [46], [25]). If the τ value changes remarkably during the acquisition of a map, it will manifests as a temperature gradient or stripes in the final image, like in Fig 6. The data from Tab 1 and 2 do not present such features, indicating that the weather conditions were stable during the observation of each map.

In order to estimate an error induced by an undetected change in the weather conditions, we decided to use the values extrapolated from the theoretical model of the SRT forecast system (see [2]) to be compared with the observed radiometer values. We derived sky opacity errors by analysing the scatter between these two different sources of sky opacity information. The final percentage error related to the sky opacity uncertainties varies in a range of 1% –1.6%.

It is worth noting that the sky opacity effects cannot be neglected in the analysis even in case of good weather conditions. Without considering the τ correction factor in the gain curve, the error induced by the opacity contribution in the QS calculation rises up to 6%.

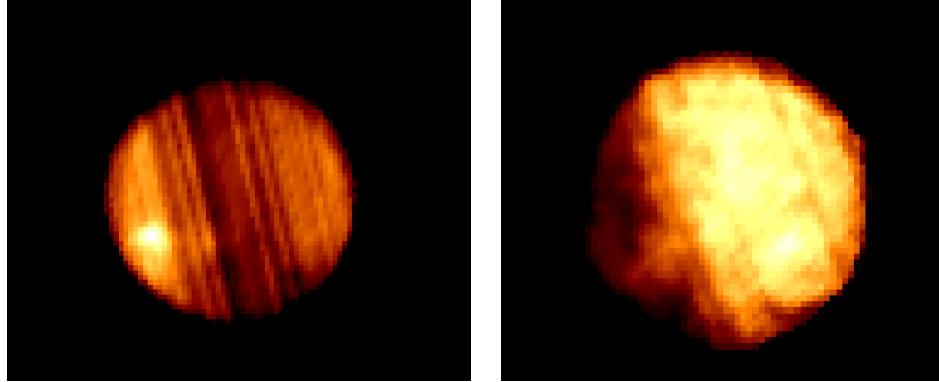


Figure 6: Examples of stripes (left panel) and temperature gradients (right panel) in a solar maps due to sudden changes in the weather conditions during the data acquisition.


5.3 Cas A spectral fit

For the Cas A spectrum expressed in equation 11, the [44] work provides a spectrum fitting of $\chi^2/(n - 4) = 0.91$, without error estimation. The measurements used in the model closest to the K-band (between about 13-33 GHz, Tab 5) are affected by an error between 0.3% and 4.2%.

Table 5: Cas A integrated fluxes ($CasA_f$) in the 13-33 GHz frequency range used in the SNR spectral fit model from [44] referred to 2015.5 epoch; ν_{obs} is the central observing frequency.

ν_{obs} [GHz]	$CasA_f(2015.5)$ [Jy]	Reference
13.5	313.0 ± 13.0	[31]
15.5	283.0 ± 12.0	[31]
16.5	273.5 ± 7.5	[31]
22.7	219.7 ± 3.0	[45]
32.9	169.4 ± 1.8	[45]
33.0	171.6 ± 0.6	[8]

We calculated the mean value, 2.3%, and used it as the relative error of the Cas A theoretical flux in the K-band. In perspective, it could be useful to perform independent flux measurements of Cas A with SRT and Medicina to better assess them in the frequency range of solar observations, without relying on the sparse literature data in K-band.

 Agenzia Spaziale Italiana	Internal Report	Document: RS-UCS-2022-007 Date: 14/09/2022 Page 22 of 35
<h2 style="text-align: center;">A New Method for Accurate Calibration of Solar Disk Emission in the Radio Band</h2>		

5.4 Secular decrease formula

To obtain the uncertainty induced by the the Eq 10 we firstly recalculated it by adding (Eq 12) and subtracting (Eq 13) the errors for each factor in the formula indicated in [44]. We used the two equations to calculate the total flux of Cas A at our epoch for both formulas. By comparing the final values, we calculated the relative error induced in the final QS value: 0.23%.

$$d_{\nu}[\%year^{-1}]_{MAX} = -(0.65) + (0.05) \ln(\nu) + (1.67) \cdot 10^{-5}(\nu)^{-2.1} \quad (12)$$

$$d_{\nu}[\%year^{-1}]_{MIN} = -(0.61) + (0.03) \ln(\nu) + (1.35) \cdot 10^{-5}(\nu)^{-2.1} \quad (13)$$

6 Calibration problems and issues

Our absolute calibration results were very stable during the first years of SunDish observations (2018-2020). However, from the beginning of 2021 we experienced some unusual and unexpected changes in our results: we found a deviation $\geq 3000K$ from the theoretical and our empirical values from Tab 4. In Tab 6 are reported the value obtained with the new observing session with the SRT through the 2021 year.

We started to investigate the possible causes for these anomalies. Our first hypothesis was a malfunction in the software caused by some changes in the code or updates. We ruled out this option by testing the same pipeline on 2019-2020 data and obtaining the same results as in Tab 4.

We can consider a possible physical origin. Semi-ARs seem to cover most of the solar disk area in some sessions. Thus, we noticed that the measured QS value could apparently fluctuate of a few hundreds K due to the increasing presence of the semi-ARs as the solar cycle is heading towards its maximum. However, the deviation shown in Tab 6 are irregular and of a thousand K from the expected values (an order of magnitude higher than semi-ARs contributions). We do not exclude a possible contribution of a more active active solar network, although, we think it is unlikely that such a sudden and remarkable change could come mostly from the relatively low-flux semi-ARs.

We then contemplated the possibility of a problem in the instrumental setups. As said previously, observing the Sun is a risky task if the instrumentation is not prepared against thermal and electromagnetic damages. The optomechanics and front-end require additional attenuation setups to guarantee instrumentation safety, ensure a linear response to the strong solar input signal impacting the systems' amplification chains and avoid electronic saturation [32]. Until the end of 2020 we verified that the typical variability of solar phenomenology in K-band was compatible with the available instrumental


 Agenzia Spaziale Italiana	Internal Report	Document: RS-UCS-2022-007 Date: 14/09/2022 Page 23 of 35
<h2 style="text-align: center;">A New Method for Accurate Calibration of Solar Disk Emission in the Radio Band</h2>		

Table 6: QS brightness levels obtained from absolute calibration procedure in year 2021. ν_{obs} is the central observing frequency; T_{QS} is the measured QS brightness temperature; Fit_{dev} expresses the percentage deviation from the expected value extrapolated from [16].

Epoch (DD/MM/YYYY)	Freq (GHz)	T_{QS} [K]	Fit_{dev} [%]
11/06/21	18.8	11986	18.4
11/06/21	24.7	11345	19.5
05/05/21	22.8	11314	17.0
05/05/21	22.8	11128	17.2
01/04/21	18.8	12883	27.3
01/04/21	24.7	11689	23.2
04/03/21	18.8	19427	91.9
04/03/21	24.7	13209	28.4
12/02/21	18.8	13126	29.7
12/02/21	24.7	13055	37.6
02/02/21	18.8	13065	29.1
02/02/21	18.8	13673	35.1
02/02/21	24.7	13528	42.5

dynamic range (see [33], [9]), as well as the calibration source Cas A. From 2021 some new strong interferences of unknown origins started to appear in our observations. The attenuation setups were adjusted to ensure the safety of the instrumentation. However, the new setups may have been too strong and the weaker SNR could have been attenuated too much, falling out from the instrumental dynamic range. In particular, an excessive signal attenuation could have lead to an underestimation of the calibration source counts, which in return produce an overestimation of the source flux, as it can be deduced from Eq 5.

Another possibility comes from the LNA deterioration. The result could be similar to that resulting from an excessive attenuation setup, with an overestimation of the target source signal. We also verified if these phenomena were connected to the observing elevation. We did not find a clear correlation with the anomalies.

In summary, it is plausible that the apparent QS excess temperature during 2021 could be due to a combination of a not optimal attenuation setup and LNA deterioration, with a possible minor contribution of the increasing network solar activity. New observations are needed to confirm our hypothesis.

6.1 Early Spectro-Polarimetric Observations at Medicina

A first opportunity to shed some light to the 2021 calibration anomalies with SRT comes with the new observations made at the Medicina Radio telescope with SARDARA ([23]), the same back-end used for solar imaging at SRT. It is worth noting that before this new implementation, Medicina provided Total-Power solar observations, contributing to most part of the [32] solar catalog. Unfortunately, these data did not allowed us to perform absolute calibration due to the relatively limited dynamic range in the Total-Power configuration.

A preliminary analysis of the new Medicina spectro-polarimetric data provided some interesting results from an absolute calibration of a solar map (Fig 7 left panel) acquired on the 28/06/2022 at 18.7 GHz (Tab 7). For this observing session we carefully selected a set of conservative attenuation parameters in order to guarantee a linear response in the lower part of the dynamic range (including Cas A flux).

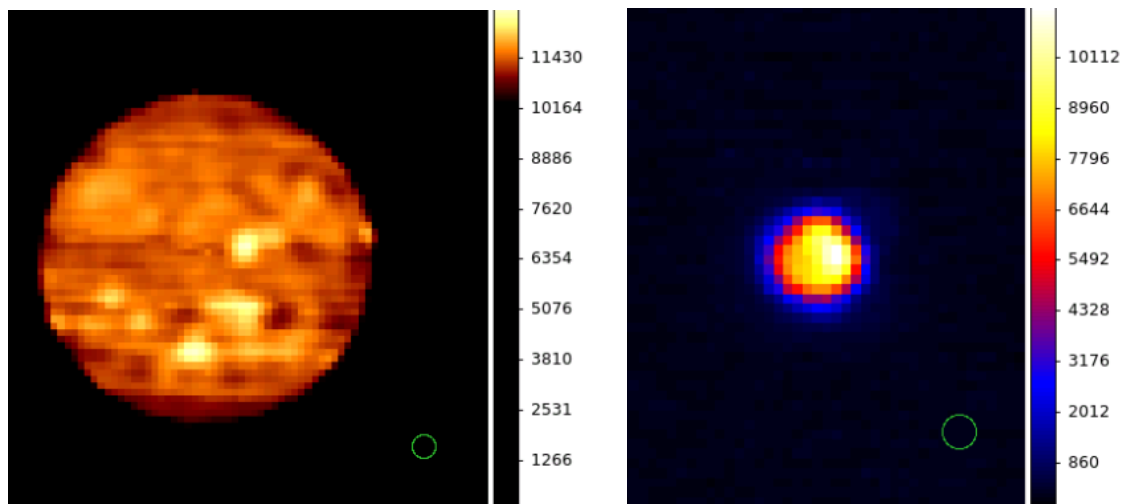


Figure 7: Sun (left) and Cas A (right) images acquired with Medicina on 28/06/2022 at 18.7 GHz with SARDARA back-end. The color bar in the solar map (left panel) is expressed in Kelvin, while the one for Cas A (right panel) is in counts. Both maps have 0.6 arcmin resolutions. The green circle represents the Medicina beam: 2.01 arcmin.

The first thing we noticed was the almost perfect accordance with the [16] fit for the right circular polarization channel, which we did not see in the 2021 data acquired with SRT. This results strengthen the hypothesis that most problems in the 2021 SRT observing sessions could be related to LNA deterioration and/or a not optimal configuration of the attenuation setups.


 Agenzia Spaziale Italiana	Internal Report	Document: RS-UCS-2022-007 Date: 14/09/2022 Page 25 of 35
<h2 style="text-align: center;">A New Method for Accurate Calibration of Solar Disk Emission in the Radio Band</h2>		

Table 7: QS brightness levels obtained from absolute calibration procedure with data acquired with the Medicina Radio Telescope on the 28/06/2022 at 18.7 GHz. T_{QS} is the measured QS brightness temperature; Fit_{dev} expresses the percentage deviation from the expected value extrapolated from [16].

Channel	T_{QS} [K]	Fit_{dev} [%]
Left circular polarization	11527	13.7
Right circular polarization	10085	0.5
Total Intensity	10806	6.6

The left circular polarization channel presents a deviation $> 10\%$, which is less than any result shown in Tab 6, but it still higher than the results from Tab 4. The difference with the left circular polarization could come from the LNA deterioration even at Medicina or a not ideal selection in the attenuation setups. We took into consideration a physical origin, but as we reported in sec 1, the QS is mostly thermal bremsstrahlung in LTE ([38]) and as stated in [4], this emission mechanism has a near zero circular polarization. We can consider the semi-AR from [13], however we still have not enough evidence to support this hypothesis.

This result comes from only one map, therefore is not enough to reach a definitive conclusion, but it contains precious information to help us in planning new observing sessions.


7 Conclusions and Future Strategies

In this work we obtained unprecedented and very precise calibrated measurements of the QS in the K-band with an error of $\sim 3\%$. This result can be further improved by new observation campaigns and the refinement of the procedures described in this note.

Through an accurate error analysis we verified the trustworthiness of the SNR Cas A as a solar calibrator, provided that the amplification chain is properly working, the attenuation setups are correctly selected and the source is within the instrument dynamic range.

This is an extremely important results, since Cas A could be one of the few calibration source visible at higher frequencies where the opacity has an even greater impact on the map quality. In the future we are also planning to go lower than 10 GHz in frequency where the [16] fit is not anymore valid, therefore the absolute calibration with Cas A will be even more crucial to obtain the physical information we need for our studies.

Among future SRT/SDSA solar configurations, observing capabilities at new frequency bands will be implemented, simultaneously covering the X (8 – 9 GHz) and K (25.5 – 27.0 GHz) or X and Ka (31

 Agenzia Spaziale Italiana	Internal Report	Document: RS-UCS-2022-007 Date: 14/09/2022 Page 26 of 35
<h2 style="text-align: center;">A New Method for Accurate Calibration of Solar Disk Emission in the Radio Band</h2>		

– 33 GHz) bands in order to fill the observational gap in literature and contributing to Space Weather networks. Moreover, together with the new SRT receivers in Q-band (33 – 50 GHz) and W-band (75 – 116 GHz), whose operations are expected to start in 2023, they could be crucial to better constrain the frequency range of ARs gyro-resonance emission [32].

For our future observing sessions and analysis we will pay particular attention to the critical aspects we identified during these years:

- we will try different attenuation setups and determine the ideal parameters to include into the instrument dynamic range both the strong and weak sources;
- at present SRT is under extraordinary maintenance due to major upgrades⁷. In the near future, the SRT and Medicina Radio Telescope LNA will be replaced. We will then be able to study the impact their deterioration had on our maps;
- we plan to make other observing sessions with the aim to obtain new calibrated QS measurements and examine the possible contribution of the semi-ARs in the results;


We will also investigate new possible anomalies and error sources, like the QS flux contributions from the beam secondary lobes in presence of strong ARs that were absent during the solar minimum, but could become more important with the raising solar activity.

⁷http://www.ponricerca.gov.it/comunicazione/esempi-di-progetto/potenziamento-infrastrutture-di-ricerca/srt_highfreq-potenziamento-del-sardinia-radio-telescope-per-lo-studio-delluniverso-alle-alte-frequenze-radio/

 <p>Agenzia Spaziale Italiana</p>	<p>Internal Report</p>	<p>Document: RS-UCS-2022-007 Date: 14/09/2022 Page 27 of 35</p>
<p>A New Method for Accurate Calibration of Solar Disk Emission in the Radio Band</p>		

Acknowledgement

S.M. acknowledges contributions from the Italian Space Agency for ASI/Cagliari University grants no. N. 2019-13-HH.0 and no. 2020-34-HH.0.


 Agenzia Spaziale Italiana	Internal Report	Document: RS-UCS-2022-007 Date: 14/09/2022 Page 28 of 35
<h2 style="text-align: center;">A New Method for Accurate Calibration of Solar Disk Emission in the Radio Band</h2>		

Contents of Figures

1	Example of a Sun and a Cas A images acquired with SRT at 18.8 GHz on 09/10/2019.	10
2	Synchronization problems of the celestial coordinate for some pixels outside the map boundaries in a Cas A image acquired on the 28/01/2020 at 18.8 Ghz.	11
3	Left panel: Total intensity map of the solar disk at 18.3 GHz acquired with the Medicina Radio Telescope on 23-Jun-2018. Right panel: histogram of brightness distribution among pixels of the solar map and estimation of the average counts from the QS using a Gaussian fit (orange line) (credits [32]).	13
4	SRT value obtained with the absolute calibration procedure (asterisks) compared to the [16] fit (red line).	18
5	comparison of different extracting regions on the same Cas A map (29/10/2020 at 18.8 GHz, Feed 0 left circular polarization): left panel a standard region from 3, right panel a region with as much background as possible.	20
6	Examples of stripes (left panel) and temperature gradients (right panel) in a solar maps due to sudden changes in the weather conditions during the data acquisition.	21
7	Sun (left) and Cas A (right) images acquired with Medicina on 28/06/2022 at 18.7 GHz with SARDARA back-end. The color bar in the solar map (left panle) is expressed in Kelvin, while the one for Cas A (right panel) is in counts. Both maps have 0.6 arcmin resolutions. The green circle represents the Medicina beam: 2.01 anrcmin.	24

Contents of Tables

1	List of the solar maps acquired with SRT analysed in this work	11
2	List of the Cas A maps acquired with SRT analysed in this work	11
3	Standard selection region for each central frequency (ν_{obs}). The <i>center</i> is indicated in Right Ascension and Declination coordinates while the <i>radius</i> of the circular region is expressed in degree	17
4	QS brightness levels obtained from the absolute calibration procedure; ν_{obs} is the central observing frequency; $Cas A_f$ lists the SNR Cassiopeia A integrated fluxes (and related observation epochs); T_{QS} is the measured QS brightness temperature; Err lists the percentage and absolute error obtained after our calculations; Fit_{dev} expresses the deviation from the expected value extrapolated from [16] in percentage and in K. . .	18

 Agenzia Spaziale Italiana	Internal Report	Document: RS-UCS-2022-007 Date: 14/09/2022 Page 29 of 35
<h2 style="text-align: center;">A New Method for Accurate Calibration of Solar Disk Emission in the Radio Band</h2>		

5	Cas A integrated fluxes ($CasA_f$) in the 13-33 GHz frequency range used in the SNR spectral fit model from [44] referred to 2015.5 epoch; ν_{obs} is the central observing frequency.	21
6	QS brightness levels obtained from absolute calibration procedure in year 2021. ν_{obs} is the central observing frequency; T_{QS} is the measured QS brightness temperature; Fit_{dev} expresses the percentage deviation from the expected value extrapolated from [16].	23
7	QS brightness levels obtained from absolute calibration procedure with data acquired with the Medicina Radio Telescope on the 28/06/2022 at 18.7 GHz. T_{QS} is the measured QS brightness temperature; Fit_{dev} expresses the percentage deviation from the expected value extrapolated from [16].	25

REFERENCES

References

- [1] Costas E. Alissandrakis. Structure of the solar atmosphere: a radio perspective. Frontiers in Astronomy and Space Sciences, 7:74, October 2020.
- [2] F. Buffa, Giampaolo Serra, Pietro Bolli, Antonietta Fara, G.L. Deiana, F. Nasir, Carluccio Castiglia, and Alessandro Delitala. K-band system temperature forecast for the sardinia radio telescope, 04 2016.
- [3] Gloria Dubner and Elsa Giacani. Radio emission from supernova remnants. Astronomy and Astrophysics Review, 23:3, Sep 2015.
- [4] G. Dulk. Solar radio emissions, 2001. Online available: <http://www.austriaca.at/;internalamp;action=hilite.actionamp;Parameter=SOLAR-> Last access:23.8.2022.
- [5] E. Egron, A. Pellizzoni, M. N. Iacolina, S. Loru, M. Marongiu, S. Righini, M. Cardillo, A. Giuliani, S. Mulas, G. Murtas, D. Simeone, R. Concu, A. Melis, A. Trois, M. Pilia, A. Navarrini, V. Vacca, R. Ricci, G. Serra, M. Bachetti, M. Buttu, D. Perrodin, F. Buffa, G. L. Deiana, F. Gaudiomonte, A. Fara, A. Ladu, F. Loi, P. Marongiu, C. Migoni, T. Pisanu, S. Poppi, A. Saba, E. Urru, G. Valente, and G. P. Vargiu. Imaging of SNR IC443 and W44 with the Sardinia Radio Telescope at 1.5 and 7 GHz. , 470(2):1329–1341, September 2017.
- [6] L. I. Fedoseev and V. I. Chernyshev. The millimeter spectrum of the quiet sun. Astronomy Reports, 42(1):105–109, January 1998.
- [7] E. Flamini, L. Garramone, M. N. Iacolina, G. Parca, E. Russo, G. Valente, and S. Viviano. Deep space communication services provided by Sardinia Deep Space Antenna - SDSA: program status and capabilities - International Astronautical Conference - Adelaide (Australia) - IAC-17,B2,8-GTS.3,4,x41239. September 2017.
- [8] Yaser A. Hafez, Rod D. Davies, Richard J. Davis, Clive Dickinson, Elia S. Battistelli, Francisco Blanco, Kieran Cleary, Thomas Franzen, Ricardo Genova-Santos, Keith Grainge, Michael P. Hobson, Michael E. Jones, Katy Lancaster, Anthony N. Lasenby, Carmen P. Padilla-Torres, José Alberto Rubiño-Martin, Rafael Rebolo, Richard D. E. Saunders, Paul F. Scott, Angela C. Taylor, David Titterington, Marco Tucci, and Robert A. Watson. Radio source calibration for the Very Small Array and other cosmic microwave background instruments at around 30 GHz. , 388(4):1775–1786, August 2008.

REFERENCES

- [9] M.N. Iacolina, A. Pellizzoni, S. Righini, and et al. Testing technological and astronomical SDSA/SRT capabilities for solar and near-Sun observations - International Astronautical Congress - Washington - IAC -19,A7,2,3,x52814. October 2019.
- [10] N. L. Johnson. Bivariate distributions based on simple translation systems. Biometrika, 36(3-4):297–304, 12 1949.
- [11] N. L. Johnson. Systems of Frequency Curves Generated by Methods of Translation. Biometrika, 36(1/2):149–176, 1949.
- [12] T. Kakinuma and G. Swarup. A Model for the Sources of the Slowly Varying Component of Microwave Solar Radiation. , 136:975, November 1962.
- [13] Juha Kallunki, Merja Tornikoski, and Irene Björklund. Identifying 8 mm Radio Brightenings During the Solar Activity Minimum. , 295(7):105, July 2020.
- [14] S. R. Kane. Impulsive (flash) phase of solar flares: Hard x-ray, microwave, euv and optical observations. Symposium - International Astronomical Union, 57:105–141, 1974.
- [15] Hannu E. J. Koskinen, Daniel N. Baker, André Balogh, Tamas Gombosi, Astrid Veronig, and Rudolf von Steiger. Achievements and Challenges in the Science of Space Weather. , 212(3-4):1137–1157, November 2017.
- [16] E. Landi and F. Chiuderi Drago. The Quiet-Sun Differential Emission Measure from Radio and UV Measurements. , 675(2):1629–1636, March 2008.
- [17] Jeffrey L. Linsky. A Recalibration of the Quiet Sun Millimeter Spectrum Based on the Moon as an Absolute Radiometric Standard. , 28(2):409–418, February 1973.
- [18] S. Loru, A. Pellizzoni, E. Egron, A. Ingallinera, G. Morlino, S. Celli, G. Umana, C. Trigilio, P. Leto, M. N. Iacolina, S. Righini, P. Reich, S. Mulas, M. Marongiu, M. Pilia, A. Melis, R. Concu, F. Bufano, C. Buemi, F. Cavallaro, S. Riggi, and F. Schillirò. New high-frequency radio observations of the Cygnus Loop supernova remnant with the Italian radio telescopes. , 500(4):5177–5194, January 2021.
- [19] S. Loru, A. Pellizzoni, E. Egron, S. Righini, M. N. Iacolina, S. Mulas, M. Cardillo, M. Marongiu, R. Ricci, M. Bachetti, M. Pilia, A. Trois, A. Ingallinera, O. Petruk, G. Murtas, G. Serra, F. Buffa, R. Concu, F. Gaudiomonte, A. Melis, A. Navarrini, D. Perrodin, and G. Valente. Investigating

REFERENCES

- the high-frequency spectral features of SNRs Tycho, W44, and IC443 with the Sardinia Radio Telescope. , 482(3):3857–3867, January 2019.
- [20] M. Marongiu, A. Pellizzoni, M. Bachetti, S. Mulas, S. Righini, G. Murtas, S. Loru, E. Egron, and Iacolina M.N. A dedicated pipeline to analyse solar data with inaf radio telescopes: Sunpit (sundish pipeline tool). Technical Report 137, OA@INAF, 2022.
- [21] M. Marongiu, A. Pellizzoni, E. Egron, T. Laskar, M. Giroletti, S. Loru, A. Melis, G. Carboni, C. Guidorzi, S. Kobayashi, N. Jordana-Mitjans, A. Rossi, C. G. Mundell, R. Concu, R. Martone, and L. Nicastro. Methods for detection and analysis of weak radio sources with single-dish radio telescopes. *Experimental Astronomy*, 49(3):159–182, May 2020.
- [22] M. Marongiu, A. P. Pellizzoni, S. Mulas, and G. Murtas. A python approach for solar data analysis: Sundara (sundish active region analyser), preliminary development. Technical Report 81, OA@INAF, 2021.
- [23] A. Melis, R. Concu, A. Trois, A. Possenti, A. Bocchinu, P. Bolli, M. Burgay, E. Carretti, P. Castangia, S. Casu, C. Cecchi Pestellini, A. Corongiu, N. D’Amico, E. Egron, F. Govoni, M. N. Iacolina, M. Murgia, A. Pellizzoni, D. Perrodin, M. Pilia, T. Pisanu, A. Poddighe, S. Poppi, I. Porceddu, A. Tarchi, V. Vacca, G. Aresu, M. Bachetti, M. Barbaro, A. Casula, A. Ladu, S. Leurini, F. Loi, S. Loru, P. Marongiu, P. Maxia, G. Mazzearella, C. Migoni, G. Montisci, G. Valente, and G. Vargiu. SARDARIA Roach2-based Digital Architecture for Radio Astronomy (SARDARA). *Journal of Astronomical Instrumentation*, 7(1):1850004, March 2018.
- [24] F. T. Nasir, C. Castiglia, F. Buffa, G. L. Deiana, A. Delitala, and A. Tarchi. Weather forecasting and dynamic scheduling for a modern cm/mm wave radiotelescope. *Experimental Astronomy*, 36(1-2):407–424, August 2013.
- [25] A. Navarrini, L. Olmi, R. Nesti, P. Ortu, P. Marongiu, A. Orlati, A. Scalambra, A. Orfei, J. Roda, A. Cattani, S. Leurini, F. Govoni, M. Murgia, E. Carretti, D. Fierro, and A. Pellizzoni. Feasibility study of a w-band multibeam heterodyne receiver for the gregorian focus of the sardinia radio telescope. *IEEE Access*, 10:26369–26403, 2022.
- [26] A. Navarrini, A. Orfei, R. Nesti, G. Valente, S. Mariotti, P. Bolli, T. Pisanu, J. Roda, L. Cresci, P. Marongiu, A. Scalambra, D. Panella, A. Ladu, A. Cattani, L. Carbonaro, E. Urru, A. Cremonini, F. Flocchi, A. Maccaferri, M. Morsiani, and M. Poloni. The sardinia radio telescope front-ends. In *27th International Symposium on Space Terahertz Technology, ISSTT 2016*, 2017.

REFERENCES

- [27] A. Nindos, C. E. Alissandrakis, G. B. Gelfreikh, V. M. Bogod, and C. Gontikakis. Spatially resolved microwave oscillations above a sunspot. , 386:658–673, May 2002.
- [28] Alexander Nindos. Incoherent Solar Radio Emission. *Frontiers in Astronomy and Space Sciences*, 7:57, November 2020.
- [29] A. Orfei, L. Carbonaro, A. Cattani, A. Cremonini, L. Cresci, F. Fiacchi, A. Maccaferri, G. Maccaferri, S. Mariotti, J. Monari, M. Morsiani, V. Natale, R. Nesti, D. Panella, M. Poloni, J. Roda, A. Scalambra, and G. Tofani. A Multi-Feed Receiver in the 18 to 26.5 GHz Band for Radio Astronomy. *IEEE Antennas and Propagation Magazine*, 52(4):62–72, August 2010.
- [30] S. Orlando, M. Miceli, M. L. Pumo, and F. Bocchino. MODELING SNR CASSIOPEIA a FROM THE SUPERNOVA EXPLOSION TO ITS CURRENT AGE: THE ROLE OF POST-EXPLOSION ANISOTROPIES OF EJECTA. *The Astrophysical Journal*, 822(1):22, apr 2016.
- [31] Creidhe O’Sullivan and D. A. Green. Constraints on the secular decrease in the flux density of CAS A at 13.5, 15.5 and 16.5 GHz. , 303(3):575–578, March 1999.
- [32] A. Pellizzoni and M. Marongiu S. Mulas G. Murtas G. Valente E. Egron M. Bachetti F. Buffa R. Concu G. L. Deiana S. L. Guglielmino A. Ladu S. Loru A. Maccaferri P. Marongiu A. Melis A. Navarrini A. Orfei P. Ortu M. Pili T. Pisanu G. Pupillo A. Saba L. Schirru G. Serra C. Tiburzi A. Zanichelli P. Zucca M. Messerotti Righini, M. N. Iacolina. Solar Observations with Single-Dish INAF Radio Telescopes: Continuum Imaging in the 18–26 GHz Range. *Solar Physics*, July 2022.
- [33] A. Pellizzoni, S. Righini, G. Murtas, F. Buffa, R. Concu, E. Egron, M. N. Iacolina, S. Loru, A. Maccaferri, A. Melis, A. Navarrini, A. Orfei, P. Ortu, T. Pisanu, A. Saba, G. Serra, G. Valente, A. Zanichelli, P. Zucca, and M. Messerotti. Imaging of the solar atmosphere in the centimetre-millimetre band through single-dish observations. *Nuovo Cimento C Geophysics Space Physics C*, 42(1):9, January 2019.
- [34] R. A. Perley and B. J. Butler. An Accurate Flux Density Scale from 50 MHz to 50 GHz. , 230(1):7, May 2017.
- [35] Christina Plainaki, Marco Antonucci, Alessandro Bemporad, Francesco Berrilli, Bruna Bertucci, Marco Castronuovo, Paola De Michelis, Marco Giardino, Roberto Iuppa, Monica Laurenza, Federica Marcucci, Mauro Messerotti, Livio Narici, Barbara Negri, Francesco Nozzoli, Stefano

REFERENCES

- Orsini, Vincenzo Romano, Enrico Cavallini, Gianluca Polenta, and Alessandro Ippolito. Current state and perspectives of Space Weather science in Italy. Journal of Space Weather and Space Climate, 10:6, December 2020.
- [36] I. Prandoni, M. Murgia, A. Tarchi, M. Burgay, P. Castangia, E. Egron, F. Govoni, A. Pellizzoni, R. Ricci, S. Righini, M. Bartolini, S. Casu, A. Corongiu, M. N. Iacolina, A. Melis, F. T. Nasir, A. Orlati, D. Perrodin, S. Poppi, A. Trois, V. Vacca, A. Zanichelli, M. Bachetti, M. Buttu, G. Comoretto, R. Concu, A. Fara, F. Gaudiomonte, F. Loi, C. Migoni, A. Orfei, M. Pilia, P. Bolli, E. Carretti, N. D’Amico, D. Guidetti, S. Loru, F. Massi, T. Pisanu, I. Porceddu, A. Ridolfi, G. Serra, C. Stanghellini, C. Tiburzi, S. Tingay, and G. Valente. The Sardinia Radio Telescope . From a technological project to a radio observatory. , 608:A40, December 2017.
- [37] C. L. Selhorst, A. Silva-Válio, and J. E. R. Costa. Solar atmospheric model over a highly polarized 17 GHz active region. , 488(3):1079–1084, September 2008.
- [38] K. Shibasaki, C. E. Alissandrakis, and S. Pohjolainen. Radio Emission of the Quiet Sun and Active Regions (Invited Review). , 273(2):309–337, November 2011.
- [39] Adriana V. R. Silva, Tatiana F. Laganá, C. Guillermo Gimenez Castro, Pierre Kaufmann, Joaquim E. R. Costa, Hugo Levato, and Marta Rovira. Diffuse Component Spectra of Solar Active Regions at Submillimeter Wavelengths. , 227(2):265–281, April 2005.
- [40] Michael J. Thompson. Grand challenges in the physics of the sun and sun-like stars. Frontiers in Astronomy and Space Sciences, 1, 2014.
- [41] G. Valente, P. Marongiu, A. Navarrini, A. Saba, G. Montisci, A. Ladu, T. Pisanu, M. Pili, S. Dessi, A. Uccheddu, N. Iacolina, D. Perrodin, M. Buttu, E. Egron, A. Melis, C. Tiburzi, and V. Vacca. The 7-beam S-band cryogenic receiver for the SRT primary focus: project status. In Wayne S. Holland and Jonas Zmuidzinas, editors, Millimeter, Submillimeter, and Far-Infrared Detectors and Instrumentation for Astronomy VIII, volume 9914, page 991422. International Society for Optics and Photonics, SPIE, 2016.
- [42] Giuseppe Valente, Tonino Pisanu, Alessandro Navarrini, Pasqualino Marongiu, Alessandro Orfei, Sergio Mariotti, Renzo Nesti, Juri Roda, Alessandro Cattani, Pietro Bolli, and Giorgio Montisci. The coaxial l-p cryogenic receiver of the sardinia radio telescope. IEEE Access, 10:2631–2645, 2022.

REFERENCES

- [43] Rashmi Verma, Giuseppe Maccaferri, Alessandro Orfei, Isabella Prandoni, and Loretta Gregorini. A new k-band (18-26 ghz) 7-horn multi-feed receiver: Calibration campaign at medicina 32 m dish, 2009.
- [44] E. N. Vinyaikin. Frequency dependence of the evolution of the radio emission of the supernova remnant Cas A. Astronomy Reports, 58(9):626–639, September 2014.
- [45] J. L. Weiland, N. Odegard, R. S. Hill, E. Wollack, G. Hinshaw, M. R. Greason, N. Jarosik, L. Page, C. L. Bennett, J. Dunkley, B. Gold, M. Halpern, A. Kogut, E. Komatsu, D. Larson, M. Limon, S. S. Meyer, M. R. Nolte, K. M. Smith, D. N. Spergel, G. S. Tucker, and E. L. Wright. Seven-year Wilkinson Microwave Anisotropy Probe (WMAP) Observations: Planets and Celestial Calibration Sources. , 192(2):19, February 2011.
- [46] Frank J. Wentz and Thomas Meissner. Atmospheric absorption model for dry air and water vapor at microwave frequencies below 100 ghz derived from spaceborne radiometer observations. Radio Science, 51(5):381–391, 2016.
- [47] Jr William B. Ashworth. A probable flamsteed observation of the cassiopeia a supernova. Journal for the History of Astronomy, 11(1):1–9, 1980.
- [48] PeiJin Zhang, Pietro Zucca, Kamen Kozarev, Eoin Carley, ChuanBing Wang, Thomas Franzen, Bartosz Dabrowski, Andrzej Krankowski, Jasmina Magdalenic, and Christian Vocks. Imaging of the quiet sun in the frequency range of 20–80 MHz. The Astrophysical Journal, 932(1):17, jun 2022.